

Available online at www.sciencedirect.com

jmr&t
Journal of Materials Research and Technology
www.jmrt.com.br



Original Article

Microstructural homogeneity, mechanical properties, and wear behavior of *in situ* Mg₂Si particles reinforced Al-matrix composites fabricated by hot rolling



Dongtao Wang ^{a,b}, Haitao Zhang ^{a,c,*}, Hiromi Nagaumi ^{a,b,*}, Pinfeng Jia ^d, Jianzhong Cui ^c

^a High-Performance Metal Structural Materials Research Institute, Soochow University, Suzhou, Jiangsu, 215021, China

^b Shagang School of Iron and Steel, Soochow University, Suzhou, Jiangsu, 215021, China

^c Key Laboratory of Electromagnetic Processing of Materials, Ministry of Education, Northeastern University, Shenyang, Liaoning, 110819, China

^d School of Materials Science and Engineering, University of Science and Technology Liaoning, Anshan, Liaoning, 114051, China

ARTICLE INFO

Article history:

Received 14 September 2019

Accepted 6 December 2019

Available online 26 December 2019

ABSTRACT

In situ Mg₂Si particles often show coarse and irregular morphologies in Al-matrix composites, which results in inhomogeneous microstructures and poor mechanical properties. This leads to poor deformation ability in Mg₂Si particles reinforced Al-matrix composites. Herein, a refined process exploiting refined Mg₂Si particles was developed to enhance microstructure homogeneity after hot rolling in an Al-11.73%Mg-6.63%Si composite. The hot-rolled sheet reduces the macroscopic cracking on the edge when the Mg₂Si particles of the as-cast microstructure are refined by the addition of phosphorus. The refined Mg₂Si particles in the as-cast state shows further size reduction and exhibits homogeneous distribution by hot rolling (reduction of 76%). The microstructure also shows uniform deformation zones, subgrains and high-density dislocation regions via hot rolling. The homogeneous deformation microstructure results in needle-like, high-density precipitates after artificial aging and decreases the stress concentration of load bearing, which is beneficial to the tensile properties and wear resistance of the composite. The wear behavior of the composites improves with Mg₂Si-particle refinement and microstructural homogeneity.

© 2019 The Authors. Published by Elsevier B.V. This is an open access article under the CC BY-NC-ND license (<http://creativecommons.org/licenses/by-nc-nd/4.0/>).

* Corresponding author at: High-Performance Metal Structural Materials Research Institute, Soochow University, Suzhou, Jiangsu 215021, China.

E-mails: haitao.zhang@epm.neu.edu.cn (H. Zhang), zhanghai888jp@suda.edu.cn (H. Nagaumi).

<https://doi.org/10.1016/j.jmrt.2019.12.020>

2238-7854/© 2019 The Authors. Published by Elsevier B.V. This is an open access article under the CC BY-NC-ND license (<http://creativecommons.org/licenses/by-nc-nd/4.0/>).

1. Introduction

Mg_2Si can act as a reinforcing phase in Al-matrix composites due to its high hardness ($4.5 \times 10^9 \text{ Nm}^{-2}$), low density ($1.99 \times 10^3 \text{ Kgm}^{-3}$), low coefficient of thermal expansion and high elastic modules [1–6]. However, coarse and irregular Mg_2Si particles diminish the tensile properties and wear resistance of the composite [7,8]. Coarse Mg_2Si particles can be refined by adding alloying elements, such as Y [9], Sb [10], Sr [11,12], Ca [13,14] and Si [15]. These alloying elements can transform the morphology and decrease the Mg_2Si particle size. Moreover, P can stably refine the Mg_2Si particles by forming the phosphide heterogeneous nucleation of primary Mg_2Si in the Al melt, where the primary Mg_2Si becomes polyhedral from its original state as irregular and dendritic. The refinement and morphology change of primary Mg_2Si improves the mechanical properties of the Al- Mg_2Si composite [16,17]. However, Mg_2Si particles often show agglomeration in the Al-matrix even if the particles are refined. The inhomogeneity of the microstructure aggravates the stress concentration at the load-bearing particles and decreases the mechanical properties of the composite.

Extrusion and hot-rolling can lead to Mg_2Si particle fragmentation, breaking of the eutectic network, recrystallized microstructures, decreasing casting defects and improvement of the particle-matrix interfaces [18–28], which can improve the yield strength (YS), ultimate tensile strength (UTS), and elongation (EL) of the Al- Mg_2Si composite. The microstructure recrystallization can also be retarded in heavily rolled Al- Mg_2Si composites [22,23]. However, in previous works, the primary Mg_2Si particles showed a non-uniform distribution in the Al-matrix, after the Al- Mg_2Si composite was extruded. This occurred even if the Mg_2Si particles were refined before the extrusion. Moreover, sheet formability of the Al- Mg_2Si composite is poor and macro-cracking often shows in the hot-rolled composite. The macro-cracking and non-uniform distribution of Mg_2Si particles in the sheet is detrimental to the mechanical properties and application of the composite. In this study, the combination of P refinement and multi-pass hot rolling can improve the homogeneity of Mg_2Si distribution, which can also improve the formability of the rolled sheet and reduce the macro-cracking. The whole treatment process shows high levels of applicability to the Al-matrix composite sheet preparation in industry.

Tribological characterization is important for extensive application of the particle-reinforced composites. The wear performance of an Al- Mg_2Si composite is crucial on the application of wear-resistant material because of the presence of rigid Mg_2Si reinforced phase. Much effort has indicated that the refinement of Mg_2Si particles can improve the wear resistance of the composite [29–31]. But now the hot-rolled and T6 treated Al- Mg_2Si composites need much more experimental work to study the wear performance, wear mechanism and accumulated energy dissipation in the dry sliding process. The T6 treatment has the potential to strengthen hot-deformed Al- Mg_2Si composites due to the precipitation strength of the β' phase. Therefore, the purpose of this paper is to improve the microstructure homogeneity using P refinement, heat treatment and multi-pass hot rolling. Moreover, the effects of

Table 1 – Chemical compositions (wt.%) of the prepared A and B composites.

	Mg	Si	P	Fe	Cr	Ti	Zn
A	11.37	6.63	0	0.02	0.02	0.01	0.03
B	11.37	6.63	0.05	0.02	0.02	0.01	0.03

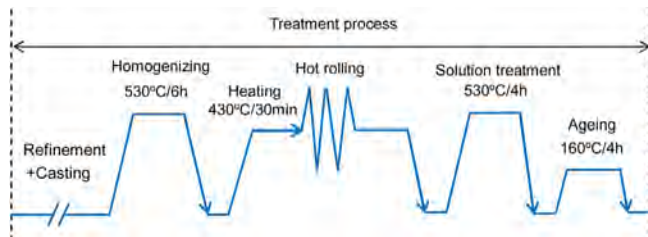


Fig. 1 – Schematic showing the technological process.

microstructure homogeneity and T6 treatment on the tensile properties and wear performance of the composite have also been investigated.

2. Experimental procedures

The chemical compositions (wt.%) of the prepared A and B composites are shown in Table 1. Commercially pure Al (99.9 wt%), pure Mg (99.9 wt%), Al-50 wt.% Si and Al-4.5 wt.% P master alloys were used to prepare the A and B composites in a 100 kW intermediate frequency furnace. The raw materials were supplied by Jiabei metals co. LTD in China. First, the Al-50 wt.% Si alloy, pure Al, and pure Mg were melted in a graphite crucible. Subsequently the melt was heated to 800 °C and held for 10 min. Degassing was conducted on the melt at 780 °C for 3 min, following a slag-removing. Afterwards, 0.05 wt.% P was added into the melt at 760 °C. The melt was stirred about 3 min to ensure proper mixing in the melt. Finally, the melt was poured into a copper mould (25 × 100 × 200 mm) to form an as-cast (AC) ingot.

Fig. 1 shows the details of the used experimental process. After refinement and casting, the hot rolling was performed on the homogenized specimens (530 °C for 6 h). Specimens with dimensions of 25 × 100 × 150 mm were cut from the composite ingot for hot rolling (H-R). The specimens were heated at 430 °C for 30 min, and then rolled to a final thickness (76% reduction with 7 passes) followed by air cooling. The hot-rolled sheets were subjected to T6 treatment (H-R & T6). The solution treatment was performed at 530 °C for 4 h followed by water quenching (25 °C). Artificial aging was carried on at 160 °C for 4 h.

Specimens were cut from the solidified ingots and hot-rolled sheets for microstructural observation. After etching with 1% HF, the microstructures were observed on a Leica DMR optical microscope. The morphologies of the eutectic Mg_2Si were examined on a Zeiss ULTRA PLUS Field Emission Scanning Electron Microscope (FE-SEM). The precipitates in the composites were observed on a FEI TECNAL G²20 type transmission electron microscope (TEM) at a voltage of 200 kV. ImagePro plus software was used to analyze the size of the

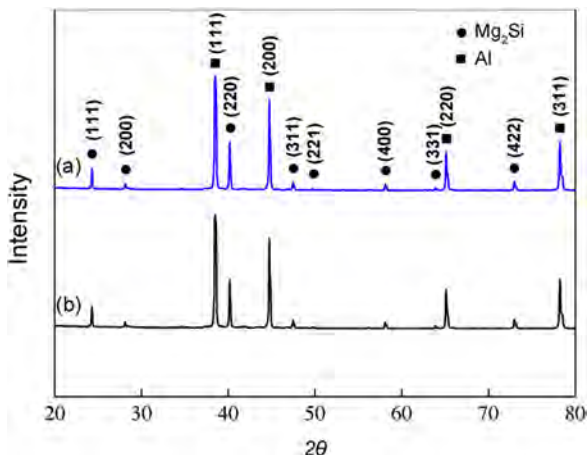


Fig. 2 – XRD patterns of (a) A composite, (b) B composite.

primary Mg_2Si particles. The diffraction peaks in the as-cast alloys were examined by X-ray diffraction (XRD) with $CuK_{\alpha 1}$ radiation by using PW3040/60X diffractometers.

A Vickers hardness tester produced by Wolpert Wilson Instruments was used to measure the hardness of the specimens (load: 5 kg; time: 10 s). Each specimen was measured at least eight random places on the surface of the specimens. The tensile test specimens were machined according to the ASTM B557M standard. The tensile test was conducted on a SHIMADZU AG-X100 kN tensile machine, with the cross head speed of 1 mm/min. Each test was measured from eight tensile specimens to obtain the average tensile properties.

Dry sliding conditions were performed to test the wear resistance of the composite (at room temperature); a pin-on-disk wear testing apparatus was used according to the ASTM G99 standard procedure. The hardness of the counter face of the steel disk is 60 HRC. The cylindrically shaped pins (diameter: 5 mm; length: 14 mm) were prepared and cleaned by ultrasonic cleaning. Five tests were measured for all the tested composites to ensure statistical accuracy.

The test parameters of all specimens were: the normal load is 100 N, the sliding speed is 200 rpm, the sliding distance is 200 m, the track radius of the rotating disk is 20 mm, and the ambient temperature is 25 °C. The wear resistance was estimated by weight loss, friction coefficient, and wear rate. The average weight loss was obtained by a microbalance (accuracy 0.01 mg). The friction coefficient was obtained by dividing the measured friction force by the applied load. The morphologies of the worn surfaces were observed by scanning electron microscopy to discuss the wear mechanisms.

3. Results and discussion

3.1. Microstructural studies

Figs. 2(a) and (b) shows the XRD results of A and B composites. Both composites consist of only Al and Mg_2Si phases. The microstructure consists of primary Mg_2Si , eutectic Mg_2Si and α -Al matrix.

The macro-photographs of the hot-rolled specimens demonstrate that the A composite exhibits more significant macroscopic cracking at the edge compared to the particle-refined B specimen, as shown in Fig. 3(a). Overall, the hot-rolled B specimen has better sheet quality. The addition of P adequately refines the Mg_2Si particles in the as-cast microstructure (Fig. 3(b) and (e)). The Mg_2Si particles show the agglomeration zones in the A composite. However, the refinement of Mg_2Si particles does not effectively alleviate the agglomeration of particles in the as-cast microstructure.

After the homogenization and hot rolling, the refined Mg_2Si particles achieve homogeneous distribution in the B composites. However, the Mg_2Si particles still show some agglomeration zones in the A composite (Fig. 3(c) and (f)). Fig. 3(d) shows the etched microstructure of the A composite after hot rolling. These results that the deformation zone of the hot-rolled A composite is inhomogeneous, and the coarse Mg_2Si particles are disordered in the deformation zone. Fig. 3(g) shows that the refined Mg_2Si particles exhibit homogeneous distribution in the uniform deformation zone.

Phosphorus addition decreases the size of the Mg_2Si particles and changes the morphology to a regular polyhedron, as shown in Fig. 4(a) and (d). The Mg_2Si particles spheroidize and refine during the subsequent homogenizing treatment and hot rolling. The hot-rolled B composite shows more uniform spheroidized Mg_2Si particles after the hot rolling in Fig. 4(g). Moreover, the eutectic Mg_2Si also spheroidize after the homogenizing treatment in the A and B composites. After the hot rolling, it is noted that the spheroidized eutectic Mg_2Si has a coincident arrangement parallel to the rolling direction (Fig. 3(h)) and exhibits homogeneous distribution (Fig. 4(g)) in the B composite. In contrary, the spheroidized eutectic Mg_2Si randomly distributes and shows the discrepancy in the size and morphology (Fig. 4(c)) in the A composite. It is evident that the B composite deforms homogeneously during the hot rolling due to the abundant refinement of Mg_2Si particles. The increased quantity, decreased size, and regular morphology of Mg_2Si particles promote the homogeneous deformation process and reduce the hindering of homogeneous deformation caused by the coarse and irregular Mg_2Si particles.

The variation of primary Mg_2Si size of the A and B composites are shown in Fig. 5(a) and (b). It can be observed that the Mg_2Si particles are larger in the as-cast and hot-rolled A composites compared with those of the B composites. After hot rolling, the Mg_2Si particle sizes decrease in the A and B composites. As seen in Fig. 4(b) and (f), the irregular Mg_2Si particles (blue zone) fragment after hot rolling.

The microstructure transformation schematics of the A and B composites are shown in Fig. 6. The homogenization treatment smooths the sharp angles of primary Mg_2Si particles; it also breaks the eutectic Mg_2Si network. Subsequently, the hot rolling procedure fragments the primary Mg_2Si into smaller particles and changes the eutectic Mg_2Si distribution. In the B composite, finer Mg_2Si particles are more freely change location in the Al matrix during hot rolling, resulting in a homogeneous distribution.

The A and B composites exhibit dislocation-tangled subgrains (yellow zones) and recrystallization (blue zones) after hot rolling due to deformation and dynamic recrystallization. The dislocation-tangled subgrains in the B composite are

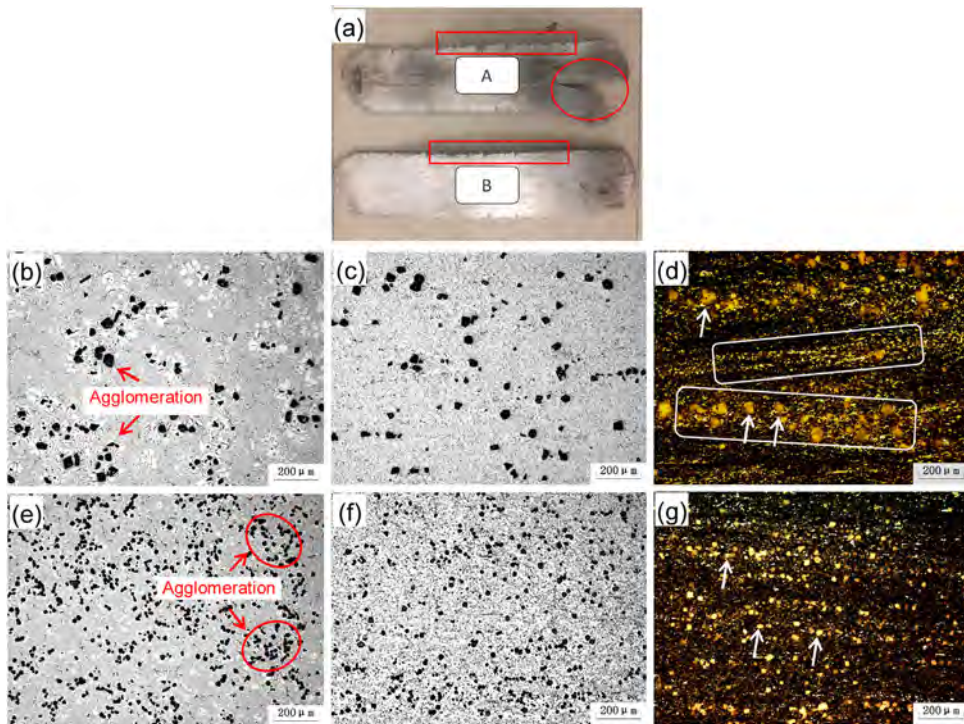


Fig. 3 – (a) Macro-photograph of hot-rolled specimens; microstructure of the A composite specimens: **(b)** as-cast; **(c)** hot-rolled; **(d)** microstructure etched by 1%HF; microstructure of the B composite specimens: **(e)** as-cast; **(f)** hot-rolled; **(g)** microstructure etched by 1%HF.

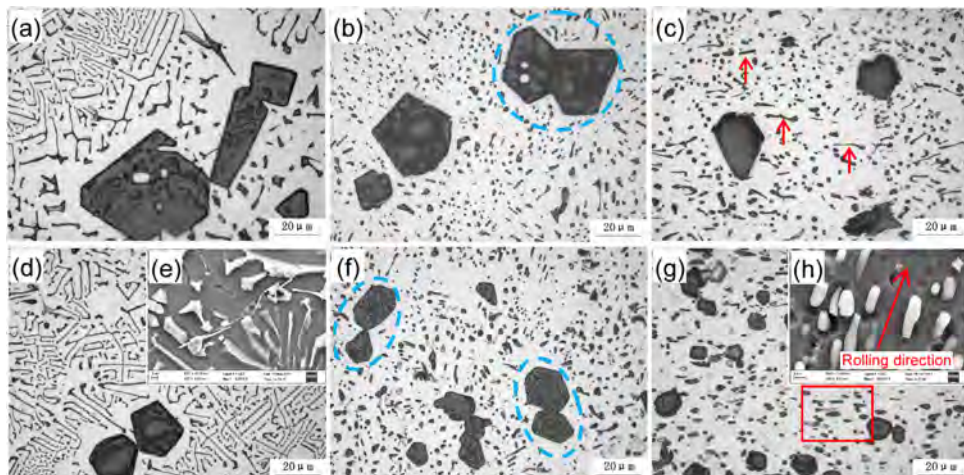


Fig. 4 – Morphologies of primary and eutectic Mg₂Si of the A composite: **(a)** as-cast; **(b)** homogenizing treatment; **(c)** hot rolling; morphologies of primary and eutectic Mg₂Si of the B composite: **(d)**, **(e)** as-cast; **(f)** homogenizing treatment; **(g)**, **(h)** hot rolling.

more homogeneous (Fig. 7(e)–(g)), and the A composite shows coarser recrystallization (Fig. 7(a)–(c)). Hot rolling results in high density dislocations. Fig. 7(b) and (d) shows the needle-like precipitations after the T6 treatment, which are finer and in higher density in the B composite. It indicates that the refinement and homogeneous distribution of Mg₂Si particles are advantage to obtain homogeneous subgrains during hot rolling.

3.2. Mechanical properties

The hardness of the AC, H-R, and H-R &T6 specimens are shown in Table 2. The as-cast A composite exhibits the lowest hardness (78.6 HV). With 0.05% P addition, the hardness of the B composite increases to 92.5 HV. Then, the B composite exhibits higher hardness after hot rolling (102.3 HV) and T6 treatment (108.8 HV). Figs. 8(a) and (b) shows the engineering stress-strain curves, UTS, YS, and EL values of the A and B

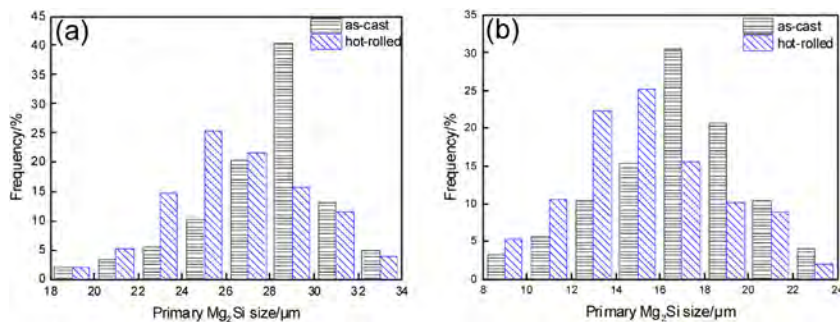


Fig. 5 – Variation of primary Mg_2Si sizes; (a) primary Mg_2Si sizes of A composite before and after the hot rolling; (b) primary Mg_2Si sizes of B composite before and after hot rolling.

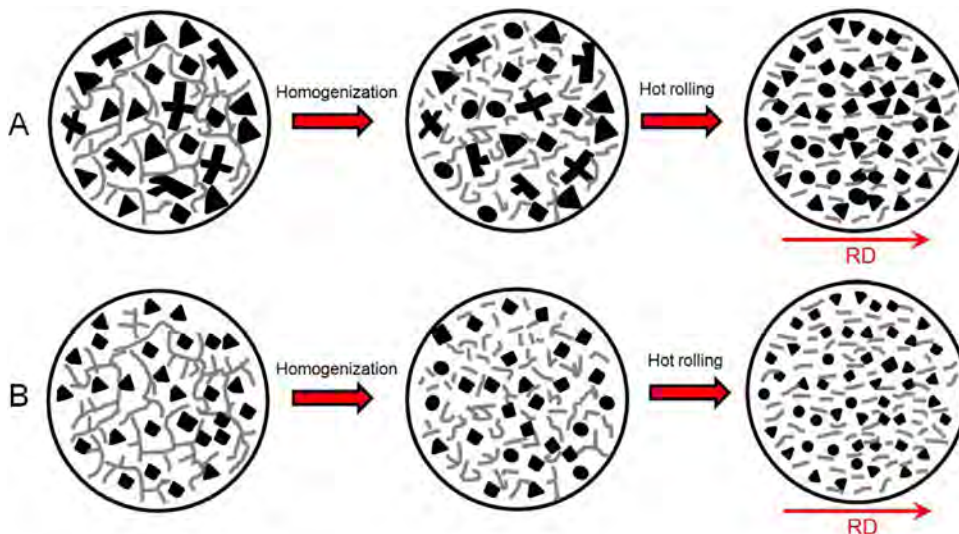


Fig. 6 – Schematic of microstructure transformation of A and B composites after homogenization and hot rolling.

Table 2 – Vickers hardness of A and B composites at various conditions.

Various conditions	AC	H-R	H-R & T6
Vickers hardness (HV)	A 78.6	B 92.5	A 84.2
	B 102.3		B 89.5
			B 108.8

composites. The tensile strengths of the hot-rolled B specimen ($YS = 179$ MPa and $UTS = 235$ MPa) are higher than that of the as-cast A specimen ($YS = 164$ MPa and $UTS = 194$ MPa) because of the Mg_2Si particles refinement and work hardening of hot rolling. The T6 heat treatment induces precipitation strengthening, resulting in YS and UTS increases to 217 and 245 MPa, respectively.

The values of EL are compared with the specimens processed by the hot rolling and T6 treatment in Fig. 8(b). Hot rolling improves the EL in the A and B composites, and the T6 treatment decreases the EL due to the needle-like precipitation.

In particle-reinforced Al matrix composites, the particle reinforcements hinder the dislocation motion and possess greater resistance to indentation [32]. The size, morphology, and distribution of reinforced particles are crucial factors to the improvement of mechanical properties in particle-

reinforced Al– Mg_2Si composites. The hardness improvement can be attributed to refinement and homogeneous distribution of the Mg_2Si particles in the P-refined and hot-rolled composites. The hot rolling process can break coarse Mg_2Si particles and ameliorate the agglomeration of Mg_2Si particles, which both improve the UTS and EL of the composite. The YS of the hot-rolled B composite is about 34 MPa higher than that of the hot-rolled A composite because of the strengthening originating from finer and homogeneous Mg_2Si particles. The high density dislocations and subgrains result in additional strengthening effects in the hot-rolled B composite. Moreover, the fragmentation and refinement of Mg_2Si particles increase the load-bearing ability in the composite. Soltani et al. reported that severe deformation and high stored strain energy resulted in strong bonding between Mg_2Si particles and Al matrix [33].

The T6 treatment improves the strength via the needle-like precipitates. The Orowan dislocation looping mechanism indicates that the precipitates can induce precipitation-strengthening, and fine and needle-like precipitates can improve the UTS and YS effectively [34,35]. In the particle-reinforced Al– Mg_2Si composites, the P refinement, hot rolling, and T6 treatment are excellent processes for the refinement of Mg_2Si particles and the tensile strength improvement.

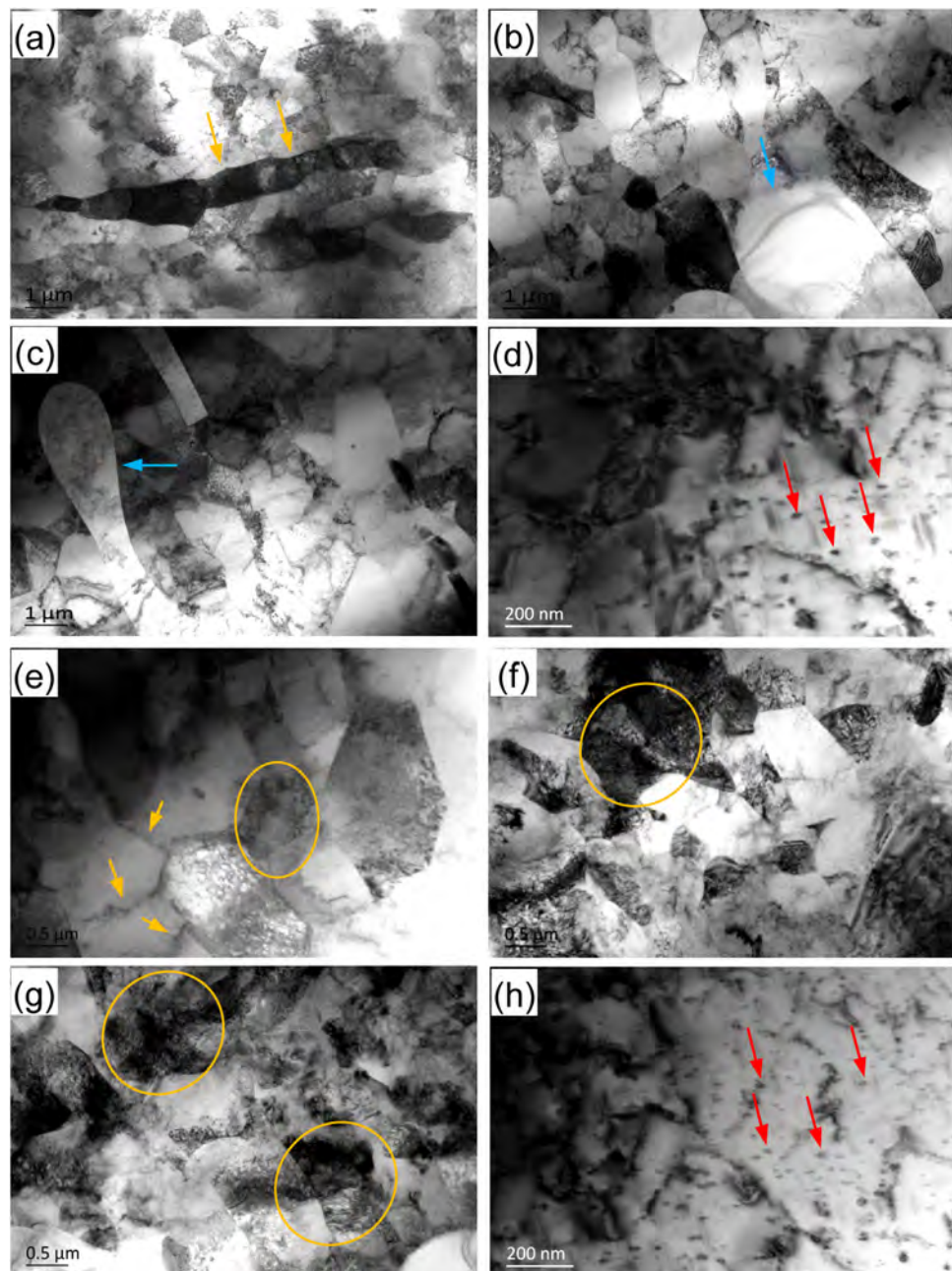


Fig. 7 – TEM images of A composite: (a), (b), (c) H-R; (d) H-R & T6; TEM images of B composite: (e), (f), (g) H-R; (h) H-R & T6.

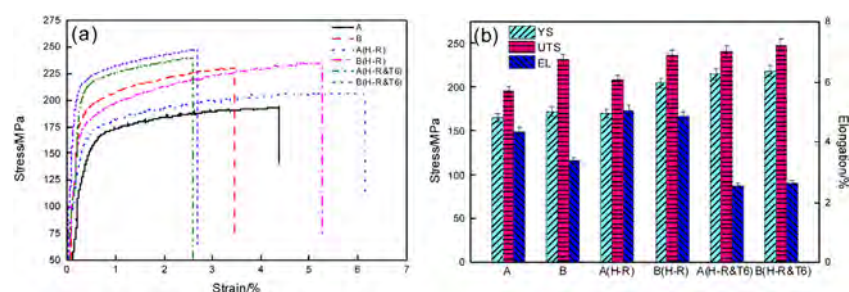


Fig. 8 – (a) Engineering stress-strain curves, (b) UTS, YS and EL of various conditions of A and B composites.

3.3. Wear behavior

The variations in weight loss for the AC, H-R and H-R &T6 specimens under loads of 100 N are shown in Fig. 9(a). These indicate that the weight loss of the B composite (6.02 mg) is less than that of the A composite (8.08 mg) in the as-cast state. Moreover, the hot rolling and T6 treatment decrease the weight loss of both A and B composites. Fig. 9(b) shows the wear rates at the different conditions. The wear rate of the B composite shows a lower value ($10.55 \text{ mm}^3/\text{km}$) compared to that ($15.54 \text{ mm}^3/\text{km}$) of the as-cast A composite in the H-R &T6 process. The decreases in wear rate and wear loss are coincident with the increased hardness discussed above.

The relationship between friction coefficient and sliding distance under applied load (100 N) are shown in Fig. 10. The friction coefficient of the as-cast A composite is higher than those of the hot-rolled composites. The friction coefficient continues to decrease in the H-R &T6 composites.

According to Archads equation [29], the wear resistance is related to material hardness:

$$Q = KW/H \quad (1)$$

where Q is the wear rate (mm^3/km), K is the wear coefficient, W is the volume of worn material per distance and H is the hardness of the specimen on the Vickers scale. This indicates that the wear rate is inversely proportional to the hardness. P addition, hot rolling, and T6 treatment resulted in the increased hardness, which enhances the wear resistance of the composite. The fine Mg_2Si particles support the contact stresses and prevent abrasion between the contact surfaces, which reduces the wear volume. The wear-resistant Mg_2Si particles dominates the wear rate of the composite. Sun and Ahlatci reported that the wear behavior of the composites is affected by type, size, and volume fraction of the reinforcement [30].

The coarse Mg_2Si particles and flake-like eutectic Mg_2Si are susceptible to cracking at the interface due to high contact stress on the tip of the irregular particles [30,31]. Crack nucleation is inclined to form at hard second-phase particles during dry sliding. These cracks are inclined to propagate on the worn surface, resulting in delamination. After hot rolling, the improved hardness leads to a higher wear resistance due to fine Mg_2Si particles and strong bonding between the Mg_2Si and Al-matrix. Previous work suggested that severe deformation (such as hot extrusion) can significantly improve the wear resistance of the as-cast composite [33]. In the H-R &T6 specimen, the weight loss, wear rate, and friction coefficient decrease due to the composite hardening. Aging strengthening results in the hardness increase and the improvement of wear resistance of the composite; it is coincident with the conclusion of Archads equation [36,37].

The worn surfaces of the AC, H-R, and H-R &T6 composites are shown in Fig. 11. Fig. 11(a) shows that the abrasion wear including delaminated areas in the as-cast A composite. During dry sliding, coarse Mg_2Si particles fracture and are pulled out from the matrix, the worn surface exhibits wide and deep ploughing grooves parallel to the sliding direction. The fragmentation of the eutectic Mg_2Si causes delamination by the stress imposed on the worn surface. Fig. 11(e) and (f) shows that the dominant wear mechanism changes to abra-

sion when the Al-18% Mg_2Si composite is subjected to the P addition, hot rolling, and T6 treatment.

In the H-R and H-R &T6 specimens of the A composite (Fig. 11(b) and (c)), abrasion and delamination are still the dominant wear mechanism. The worn surface of the H-R specimen of the B composite has a smooth appearance with shallow and narrow grooves. The improved wear resistances in the hot-rolled specimens are attributed to fine and dispersed Mg_2Si particles in the matrix. Moreover, the eutectic Mg_2Si with a rod-like shape tends to enhance the bonding with the matrix; it can effectively suppress the formation of cracks and improve the wear resistance. The wear resistance further improves due to hardening in the H-R &T6 specimen of B composite.

The schematics of the dry sliding process and corresponding worn surfaces at different conditions are shown in Fig. 12. The coarse and irregular Mg_2Si particles result in high stress concentration between the particles and Al matrix in the as-cast composite. The high stress concentration leads to particles being pulled out from the matrix and subsequent breakage of the matrix; thus the worn surface exhibits wide and deep ploughing grooves (Fig. 12(a) and (b)). With P addition, the Mg_2Si particles are refined and transform to a regular morphology. This transformation effectively reduces the stress concentration. The regular Mg_2Si particles are more difficult to be pulled out from the matrix which alleviates the breakage of the matrix. The worn surface shows less pulled particles and shallow grooves (Fig. 12(c) and (d)). When the P-refined composite was performed by the hot rolling, the Mg_2Si particles were further refined and spheroidized. The spheroidized Mg_2Si particles cause less stress concentration and improve the continuity of the matrix. The smoother worn surface indicates the higher wear resistance of the composite (Fig. 12(e) and (f)).

Friction process always remain storing and transforming of energy. Accumulated energy dissipation during dry sliding systems is also an important parameter to predict the wear behavior of the composite [38–40]. Many factors can affect the friction energy dissipation, such as an increase in contact temperature, the generation of wear particles, and plastic deformation and phase transformation [41,42]. Moreover, Sondur et al. reported that heat treatment also affected the wear behavior of particle-reinforced composites [36,37]. Ramalho et al. suggested the relationship between dissipated energy and wear; the accumulated energy dissipation can be estimated by the following equations [38–40]:

$$dE_d = F_t dx \quad (2)$$

$$E_d = \int_0^{\Delta t} F_t dx \quad (3)$$

where dE_d is the incremental dissipated energy, F_t is the friction force, dx is the incremental wear distance, and Δt is the time intervals.

The relationship between the accumulated energy dissipation (E_d) and wear volume (V_w) at different conditions is shown in Fig. 13(a). The accumulated energy dissipation increases with the increase of the wear volume. The as-cast A composite exhibits the highest accumulated energy dissipation. With the P addition, hot rolling, and T6 treatment, the accu-

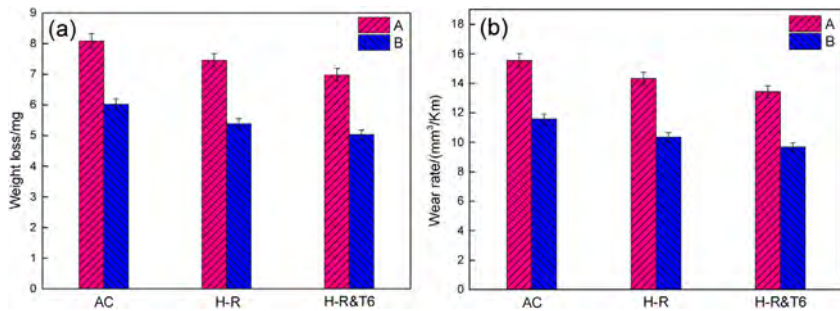


Fig. 9 – (a) Wear weight loss of various conditions of A and B composites under 100 N; (b) Wear rates of various conditions of A and B composites under 100 N.

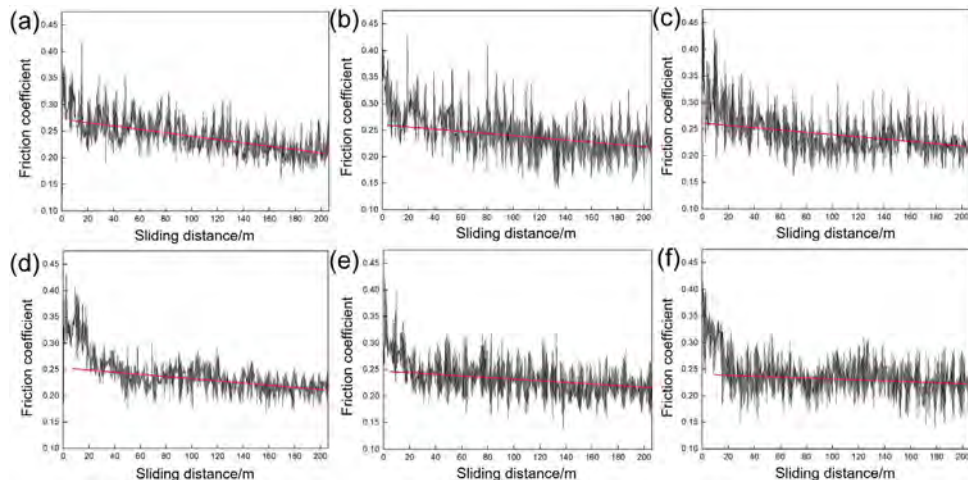


Fig. 10 – Relationship in the friction coefficient versus sliding distance: A composite (a) AC, (b) H-R, (c) H-R &T6; B composite (d) AC, (e) H-R, (f) H-R &T6.

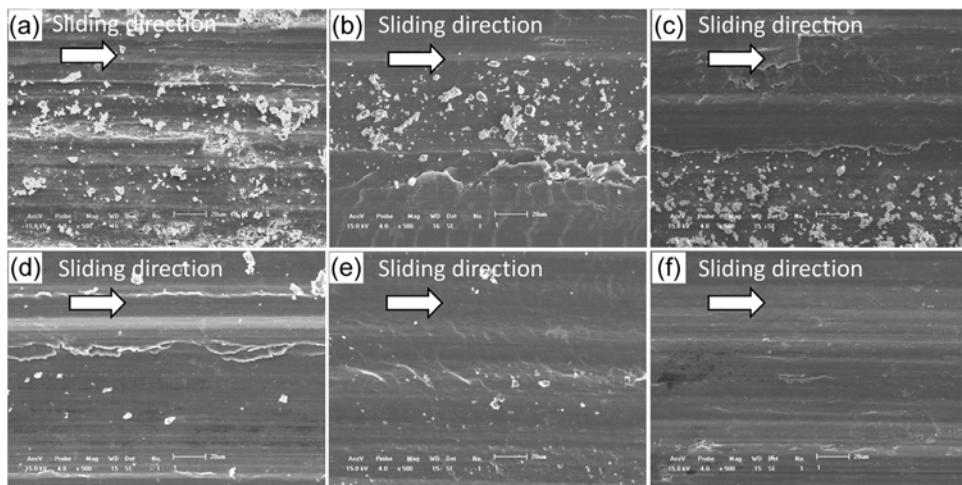


Fig. 11 – SEM images of worn surfaces under the loads of 100 N and the sliding distance of 200 m: A composite (a) AC, (b) H-R, (c) H-R &T6; B composite (d) AC, (e) H-R, (f) H-R &T6.

mulated energy dissipation gradually reduces during the dry sliding process. It can be noted that the slope of the curve is not a constant when the composite was subjected to the different treatments. Jahangiri et al. suggested that wear mode of the composite does not change if the slope of the $E_d - V_w$ curve is a constant [40]. The slope variation indicates the change of the

wear mode when the composite undergoes P-refinement, hot rolling and T6 treatment. It is coincident with the observation of the wear surfaces at different conditions.

Since the Mg_2Si particles are coarse, irregular, and aggregated in the as-cast A composite, more Mg_2Si particles crack and the Al matrix significantly scuffs, dissipating more energy

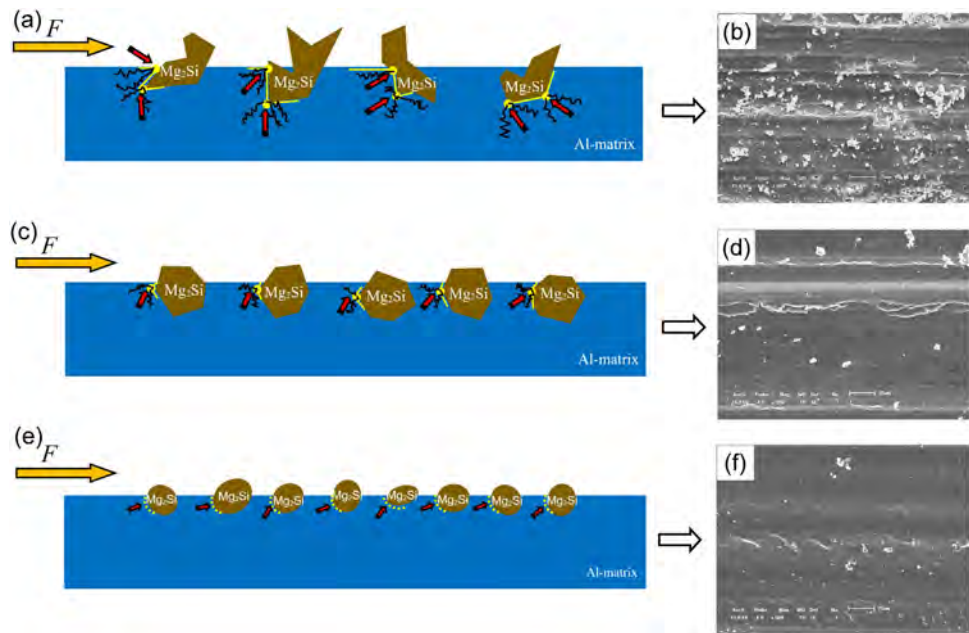


Fig. 12 – Schematic of dry sliding process and the corresponding worn surfaces at different conditions: (a), (b) as cast; (c), (d) P addition; (e), (f) hot rolling.

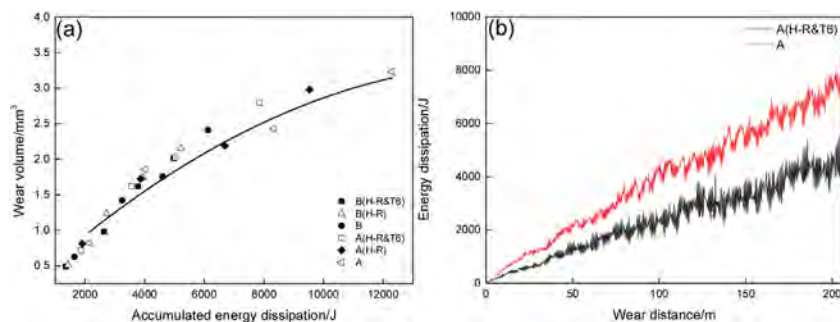


Fig. 13 – (a) The relationship between the accumulated energy dissipation (E_d) and wear volume (V_w) at different conditions; (b) the relationship between the energy dissipation and wear distance at different conditions.

in the friction process. A combination of adhesion and delamination is the dominant mechanism. The wear mode of the H-R &T6 specimen of the B composite changes to abrasion, which dissipates less energy due to the fine and dispersed Mg₂Si particles, stronger bonding of the Al matrix, and higher load-bearing ability. Fig. 13(b) indicates that the hot rolling and T6 treatment reduce the energy dissipation of the composite in the friction process. It implies less wear mass loss and stronger wear resistance due to fewer cracks.

4. Conclusions

In the present investigation, the effects of P-refinement, hot rolling, and T6 treatment on microstructure, mechanical properties, and wear behavior of Al-18 wt.% Mg₂Si in situ composites were studied. The results indicate that:

- P-refinement and hot rolling result in decreased size and dispersed distribution of Mg₂Si particles. It also has a significant effect on the breakage of the flake-like eutectic

Mg₂Si in the matrix. The P-refined composite exhibits more homogeneous particle distribution, uniform deformation zones, subgrains, and high-density dislocation regions by subsequent hot rolling. The needle-like phases precipitate in the matrix after the T6 treatment for both composites. The combination of P refinement and multi-pass hot rolling improve the formability of rolled sheet and reduce macro-cracking.

- Consequently, the hot rolling and T6 treatment improve the hardness, yield strength and ultimate tensile strength in the A and B composites. The refinement of Mg₂Si particles, subgrains, high density dislocation, and needle-like precipitates are dominant factors related to the improved mechanical properties.
- The wear resistance of the hot-rolled specimen is higher than that of the as-cast composites. The hot-rolled and T6-treated B composite exhibits the lowest weight loss and friction coefficient due to the fine Mg₂Si phases and the increased hardness. A combination of adhesion and delamination is the dominant wear mechanism in the as-cast A

composite. The wear mechanism changes to abrasion in the H-R &T6 specimen of the B composite.

Conflicts of interest

The authors declare no conflicts of interest.

Acknowledgements

The authors gratefully acknowledge the supports of the Doctoral Foundation of China Ministry of Education (Grant number 20130042130001), China Postdoctoral Science Foundation (Grant number 2019M661928), National Natural Science Foundation of China (Grant No. U1864209), 2017 joint fund of State Key Laboratory of Metal Materials and Applications for Marine Equipment and University of Science and Technology Liaoning (Grant No. SKLMEA-USTL-201704).

REFERENCES

- [1] Saffari S, Akhlaghi F. Microstructure and mechanical properties of Al-Mg₂Si composite fabricated in-situ by vibrating cooling slope. *Trans Nonferrous Met Soc China* 2018;28(4):604–12.
- [2] Biswas P, Mondal MK, Roy H, Mandal D. Microstructural evolution and hardness property of in situ Al-Mg₂Si composites using one-step gravity casting method. *Can Metall Q* 2017;56(3):340–8.
- [3] Takeuchi S, Hashimoto T, Suzuki K. Plastic deformation of Mg₂Si with the C1 structure. *Intermetallics* 1996;4(8):147–50.
- [4] He Y, Zhang H, Li T, Wang X. Calculation of Jackson's factor of Mg₂Si in Mg melt using coordination polyhedron. *J Alloys Compd* 2013;581:494–7.
- [5] Kurt H, Oduncuoglu M. Formulation of the effect of different alloying elements on the tensile strength of the in situ Al-Mg₂Si composites. *Metals* 2015;5(1):371–82.
- [6] Li C, Wu YY, Li H, Liu XF. Morphological evolution and growth mechanism of primary Mg₂Si phase in Al-Mg₂Si alloys. *Acta Mater* 2011;59(3):1058–67.
- [7] Nodoshan HRJ, Liu W, Wu G, Bahrami A, Pech-Canul MI, Emamy M. Mechanical and tribological characterization of Al-Mg₂Si composites after yttrium addition and heat treatment. *J Mater Eng Perform* 2014;23(4):1146–56.
- [8] Li GH, Gill HS, Varin RA. Magnesium silicide intermetallic alloys. *Metall Mater Trans A* 1993;24(11):2383–91.
- [9] Wang H, Zhu JN, Li J, Li C, Zha M, Wang C, et al. Refinement and modification of primary Mg₂Si in Al-20Mg₂Si alloy by a combined addition of yttrium and antimony. *CrystEngComm* 2017;19:6365–72.
- [10] Farahany S, Ghandvar H, Nordin NA, Ourdjini A. Microstructure characterization, mechanical, and tribological properties of slow-cooled Sb-treated Al-20Mg₂Si-Cu in situ composites. *J Mater Eng Perform* 2017;26(4):1685–700.
- [11] Srinivasan A, Pillai UTS, Swaminathan J, Das SK, Pai BC. Observations of microstructural refinement in Mg-Al-Si alloys containing strontium. *J Mater Sci* 2006;41(18):6087–9.
- [12] Nordin NA, Farahany S, Ourdjini A, Bakar TAA, Hamzah E. Refinement of Mg₂Si reinforcement in a commercial Al-20%Mg₂Si in-situ composite with bismuth, antimony and strontium. *Mater Charact* 2013;86(8):97–107.
- [13] Moussa ME, Waly MA, El-Sheikh AM. Effect of Ca addition on modification of primary Mg₂Si, hardness and wear behavior in Mg-Si hypereutectic alloys. *J Magnes Alloy* 2014;2(3):230–8.
- [14] Kim JJ, Kim DH, Shin KS, Kim NJ. Modification of Mg₂Si morphology in squeeze cast Mg-Al-Zn-Si alloys by Ca or P addition. *Scr Mater* 1999;41(3):333–40.
- [15] Li C, Wu Y, Li H, Liu X. Microstructural formation in hypereutectic Al-Mg₂Si with extra Si. *J Alloys Compd* 2009;477(1):212–6.
- [16] Tebib M, Samuel AM, Ajersch F, Chen XG. Effect of P and Sr additions on the microstructure of hypereutectic Al-15Si-14Mg-4Cu alloy. *Mater Charact* 2014;89(3):112–23.
- [17] Qin QD, Zhao YG, Zhou W, Cong PJ. Effect of phosphorus on microstructure and growth manner of primary Mg₂Si crystal in Mg₂Si/Al composite. *Mater Sci Eng A* 2007;447(1–2):186–91.
- [18] Bahrami A, Razaghian A, Emamy M, Khorshidi R. The effect of Zr on the microstructure and tensile properties of hot-extruded Al-Mg₂Si composite. *Mater Des* 2012;36:323–30.
- [19] Yeganeh SEV, Razaghian A, Emamy M. The influence of Cu-15P master alloy on the microstructure and tensile properties of Al-25wt%Mg₂Si composite before and after hot-extrusion. *Mater Sci Eng A* 2013;566(2):1–7.
- [20] Emamy M, Khodadadi M, Raouf AH, Nasiri N. The influence of Ni addition and hot-extrusion on the microstructure and tensile properties of Al-15%Mg₂Si composite. *Mater Des* 2013;46(4):381–90.
- [21] El-Sabbagh A, Soliman M, Taha M, Palkowski H. Hot rolling behaviour of stir-cast Al 6061 and Al 6082 alloys - SiC fine particulates reinforced composites. *J Mater Process Technol* 2012;212(2):497–508.
- [22] Tham LM, Gupta M, Cheng L. Effect of reinforcement volume fraction on the evolution of reinforcement size during the extrusion of Al-SiC composites. *Mater Sci Eng A* 2002;326(2):355–63.
- [23] Razaghian A, Bahrami A, Emamy M. The influence of Li on the tensile properties of extruded in situ Al-15%Mg₂Si composite. *Mater Sci Eng A* 2012;532(1):346–53.
- [24] Soltani N, Bahrami A, Pech-Canul MI. The effect of Ti on mechanical properties of extruded in-situ Al-15pct Mg₂Si composite. *Metall Mater Trans A* 2013;44(10):4366–73.
- [25] Fard RR, Akhlaghi F. Effect of extrusion temperature on the microstructure and porosity of A356-SiC_p composites. *J Mater Process Technol* 2007;187(4):433–6.
- [26] El-Sabbagh A, Soliman M, Taha M, Palkowski H. Hot rolling behaviour of stir-cast Al 6061 and Al 6082 alloys-SiC fine particulates reinforced composites. *J Mater Process Technol* 2012;212(2):497–508.
- [27] Hurley ND, Geertruyden WHV, Misiolek WZ. Surface grain structure evolution in hot rolling of 6061 aluminum alloy. *J Mater Process Technol* 2009;209(18–19):5990–5.
- [28] Archard JF. Contact and rubbing of flat surfaces. *J Appl Phys* 1953;24:981–8.
- [29] Sun Y, Ahlatci H. Mechanical and wear behaviors of Al-12Si-XMg composites reinforced with in situ Mg₂Si particles. *Mater Des* 2011;32(5):2983–7.
- [30] Qin QD, Zhao YG, Zhou W. Dry sliding wear behavior of Mg₂Si/Al composites against automobile friction material. *Wear* 2008;264(7–8):654–60.
- [31] Montoya-Dávila M, Pech-Canul M, Pech-Canul M. Effect of bi- and trimodal size distribution on the superficial hardness of Al/SiCp composites prepared by pressureless infiltration. *Powder Technol* 2007;176(2–3):66–71.
- [32] Soltani N, Nodoshan HRJ, Bahrami A, Pech-Canul MI, Liu W, Wu G. Effect of hot extrusion on wear properties of Al-15 wt.% Mg₂Si in situ metal matrix composites. *Mater Des* 2014;53(1):774–81.

- [34] Mehr VY, Rezaeian A, Toroghinejad MR. Application of accumulative roll bonding and anodizing process to produce Al–Cu–Al₂O₃ composite. Mater Des 2015;70:53–9.
- [35] Wang Q, Caceres C. On the strain hardening behaviour of Al–Si–Mg casting alloys. Mater Sci Eng A 1997;234(97):106–9.
- [36] Sondur DG, Goudar DM, Mallapur DG, Rudrakshi GB. Study of microstructure and wear behavior of T6 heat treated as cast Al–25Mg₂Si–2Cu alloy. Mater Sci Forum 2015;830–831:358–61.
- [37] Sameezadeh M, Emamy M, Farhangi H. Effects of particulate reinforcement and heat treatment on the hardness and wear properties of AA2024–MoSi₂ nanocomposites. Mater Des 2011;32(4):2157–64.
- [38] Ramalho A, Miranda JC. The relationship between wear and dissipated energy in sliding systems. Wear 2006;260(4):361–7.
- [39] Huq MZ, Celis JP. Expressing wear rate in sliding contacts based on dissipated energy. Wear 2002;252(5–6):375–83.
- [40] Jahangiri M, Hashempour M, Razavizadeh H, Rezaie HR. A new method to investigate the sliding wear behaviour of materials based on energy dissipation: W-25 wt%Cu composite. Wear 2012;274–275(3):175–82.
- [41] Fourny S, Paulin C, Liskiewicz T. Application of an energy wear approach to quantify fretting contact durability: introduction of a wear energy capacity concept. Tribol Int 2007;40(10–12):1428–40.
- [42] Jahangiri M, Hashempour M, Razavizadeh H, Rezaie HR. Application and conceptual explanation of an energy-based approach for the modelling and prediction of sliding wear. Wear 2012;274–275(3):168–74.